Projecting the Effects of Land Subsidence and Sea Level Rise on Storm Surge Flooding in Coastal North Carolina

Jeremy Johnston (jjohns60@gmu.edu)
George Mason University
Felicio Cassalho
George Mason University
Tyler Miesse
George Mason University
Celso Ferreira
George Mason University

Research Article

Keywords: Land Subsidence, Sea, Rise, Storm, Flooding, Coastal North Carolina, United States, ground water, ecosystems

Posted Date: June 3rd, 2021

DOI: https://doi.org/10.21203/rs.3.rs-571352/v1

Abstract

Much of the United States Atlantic coastline continues to subside due to post glacial settlement and ground water depletion. Combined with sea level rise (SLR), this contributes to a larger relative rate of SLR regionwide. In this work, we utilize the ADvanced CIRCulation model to simulate storm surges across coastal North Carolina. Simulations of recent Hurricanes Irene (2011) and Matthew (2016) are performed considering SLR projections and land subsidence estimates for the year 2100. The model is validated against historic water level observations with generally strong agreement (mean R^2 0.81, RMSE 10–31 cm). At current rates of subsidence, storm surge susceptible regions increase on the order of 30–40% by 2100 relative to near-present day conditions. Flood water redistribution leaves low-lying areas especially vulnerable, as many of which also experience increased land subsidence. Combined with SLR projections, results project more than a doubling of areal flood extent for Hurricane Irene from ~ 2,000 km^2 (2011) to 5,000 km^2 (2100, subsidence + 74 cm), and more than a 3-fold increase ~ 1,400 km^2 (2016) to 4,900 km^2 (2100, subsidence + 74 cm) for Hurricane Matthew. The expected inundation increases have substantial implications for communities and ecosystems located in coastal North Carolina.

Introduction

As much of North America experiences post-glacial rebound following the most recent ice age, large sections of the east coast of the United States continue to settle. This phenomenon occurs over the mid-latitudes, including coastal New Jersey through South Carolina, as sections of land that were forced upward (forebulge) by glacial loading to the north are now settling following the loss of ice mass [1],[2]. Groundwater extraction has also led to increased subsidence rates along the East Coast from New York to Florida [2]-[4]. Post glacial settling coupled with continued ground water extraction has resulted in comparatively rapid land movement at more than twice the long-term historical rate along large portions of the U.S. Atlantic coastline, exceeding 3 mm/year [2]. While sea-level rise (SLR) is considered a primary driver of worsening coastal flooding, the specific influences due to changes in land surface elevations, both anthropogenic and due to natural settlement, are largely overlooked. In the southern Chesapeake Bay region and across North Carolina, these rates are among the fastest on the eastern seaboard [5],[6]. This contributes to an accelerated increase in storm surge flood risk [7]-[9] and can result in tidal flooding, impair drainage systems, and increase reliance on engineered flood protection systems [10]-[12].

Still, rising sea levels remain a significant driver of coastal flooding. By 2100, even in low carbon emissions scenarios over 190 million people are expected to be vulnerable to high tide flooding alone [13],[14]. In coastal North Carolina, anticipated SLR increases range from around 0.2 m (low) to 3.0 m (extreme), with intermediate projections of SLR alone generally falling between 0.5 m and 1 m by the year 2100 [15]-[17]. As a result, large coastal communities in North Carolina and the southern Chesapeake Bay region (population > 2 million, [18]) are at increased flood risk with economic, social, and environmental implications [19]-[23]. Accumulation of several risk factors is likely to contribute to a notable increase in coastal flooding across the region in the coming decades. These include SLR, sinking ground, growing coastal populations [24],[25], and the potential for more frequent and stronger storms due to warming oceans [26]. Within the last decade alone, high-impact events such as Hurricane Irene and Matthew have directly resulted in a considerable environmental toll [27], dozens of deaths, and economic losses of an estimated $15.8 billion [28] and $10 billion [29], respectively.

Enhanced computational capabilities and numerical circulation models enable the use of computer-based tools for estimating storm surge with a high degree of accuracy [8], [30]-[32]. By perturbing model inputs, numerical modeling approaches have the capability of simulating synthetic storm events. Adjustments to storm track, storm intensity (i.e., central pressure, wind fields), land cover, water levels (i.e., SLR), and underlying digital elevation models (i.e., subsidence) can be used to simulate a wide range of scenarios. Coastal North Carolina specifically, provides a well characterized and instrumented candidate region for the use of numerical circulation models. In the region, Peng et al. [33] estimated over 500 km^2 of flooded area from a Category 3 hurricane near the mouth of the Pamlico River alone. In the neighboring Cape Fear region, the Princeton Ocean Model was effectively used to simulate storm surge dynamics by hindcasting historical storm events [34]. For Hurricane Irene (2011), Loftis et al. [8] investigated the impacts had it made landfall in 2045, predicting substantial increases in flood extent in the lower Chesapeake Bay. Other efforts to quantify the contributions of land subsidence and SLR to storm surge flooding in Shanghai have also employed numerical modeling [30]. These studies, among others, have underlined the usefulness of numerical simulation for surge prediction and risk assessment. However, the unique contributions from SLR and ongoing land settlement to future region-wide coastal flooding is not explored. Due to land movement rates that are not spatially continuous and uncertainty in SLR, it is important to assess local impacts that may otherwise be missed when considering uniform land movement or SLR. Due to rapid subsidence and an already low-lying land surface, investigation into the potentially devastating flooding in North Carolina and the southern Chesapeake Bay is increasingly valuable. Hurricanes provide a swift realization of the effects of regional changes that are in stark contrast to the steady and sometimes imperceptible inter-annual changes. Coastal storm events have the potential to bring increasingly devastating impacts to life, property, and coastal ecosystems which can illuminate the implications of persistent changes in the land surface and sea levels.

In the following sections, we investigate the effect of land subsidence and SLR in coastal North Carolina and southern Virginia with the objective to (1) quantify the increased extent of areas prone to storm surge due to predicted land movement (relative to present day conditions) and (2) to examine the relative contributions of SLR and subsidence to coastal flooding. These efforts have important implications for flood mitigation and planning of coastal resilience (e.g., zoning and engineered defenses) by projecting regional vulnerability to coastal flooding.

Methods

Study Region

Coastal North Carolina is home to a unique network of islands, bays, estuaries, and sounds that make up the Albemarle-Pamlico Estuary System (APES, Fig. 1). The region includes Pamlico Sound, a lagoon extending for 80 miles between the North Carolina mainland and the Outer Banks. The region is also home to a large tourism and agriculture industry, fisheries, and supports a considerable population [22]. The complex interplay between these components, coupled with the region wide vulnerability to storm surge flooding [35],[36] make it a challenging yet fascinating case study region for the prediction of coastal flooding. The area contains the largest saltwater lagoon on the East Coast serving both as an important fishery [37] and a critical ecosystem [38]-[40]. The barrier island chain of the Outer Banks separates the Albemarle-Pamlico Estuary System (APES) from the Atlantic Ocean to the east. These islands serve as a breakwater, greatly damping tidal influences and wave action within the APES and connect the sound to the Atlantic Ocean by the Oregon, Hatteras, and Ocracoke Inlets [41]. The region is also prone to storm surge flooding due to the regular occurrence of hurricanes (on average every ~ 2.5 years, [36]). This includes recent events such as Irene (2011), Matthew (2016), Florence (2018), and Dorian (2019) as a marked increase in hurricane activity can be shown extending from the early 1990's through the present day [26],[42].

The ADvanced CIRCulation Model

The ADvanced CIRCulation (ADCIRC) model is a hydrodynamic circulation model which uses modified shallow-water equations and a triangular mesh to model complex interactions between water bodies and the land surface [45]. Several studies have employed ADCIRC in the modeling of storm surge and wave action through coupling with the Simulating WAves Nearshore (SWAN, [46]) model which is used to describe wave evolution. The coupled ADCIRC + SWAN model was used to assess storm surge potential in the region surrounding Galveston, TX [31]. These models have also been successfully employed to study the hydrodynamic response in the Gulf of Maine during notable coastal flooding events

[47]. The North Carolina Forecasting System, developed to provide operational storm surge and wave information to decision makers, also relies on ADCIRC [48]. For this study, the ADCIRC configuration used to model storm surge over the APES region consists of a triangular mesh of over 800,000 nodes. Node elevations are determined from the underlying digital elevation model (DEM), which is derived from the U.S. Coastal Relief Model [49], the Continuously Updated Digital Elevation Model (CUDEM; [50]), and the General Bathymetric Chart of the Oceans [51]. The effects of vegetation and friction are accounted for using Manning's n roughness coefficients derived using the U.S. National Landcover Database [52] using the scheme presented by Liu et al. [53]. Atmospheric forcing data are provided in the form of wind fields and surface pressure, forced with hourly data from the European Center for Medium-Range Weather Forecasts (ECMWF ERA5, [54]) reanalysis models. Further information on the specific configuration of the coupled ADCIRC + SWAN model utilized here is presented in Cassalho et al. [32].

Subsidence Projections

Land subsidence rates are estimated based on GPS derived vertical change rates presented by Karegar et al. [2]. In this work, they examined displacement trends in GPS elevation data at 216 stations spanning from Maine to Florida down the Atlantic Coast. The study found the most rapid settlement rates occurring over Mid-Atlantic and southeastern coastal areas (up to -2.9 mm/year), while slower land movement was observed inland with large parts of the Northeast even experiencing increases land uplift. Annual rates from these stations were interpolated using natural neighbor interpolation to create a continuous map of displacement rates across the region (Fig. 2). Using a recent DEM (see section, *The ADvanced CIRCulation Model*) to create the baseline approximation for 2020 surface elevations, projected elevations for year 2100 were calculated using a linear forecast, shown in Eq. (1):

$$DEM_{2100} = DEM_{recent} + S_r(2100 - 2020) \qquad (1)$$

Where S_r represents the annual rate of land movement at a given cell in the interpolated raster. Vertical displacement projections ranged from − 23 cm to -3 cm by 2100, with the highest rates occuring within the P-AP. Overland mesh nodes in the ADCIRC model were then modified by applying the value from the nearest interpolated cell to the corresponding node elevations. Interpolated land movement rates were not applied to mesh nodes below sea level due to uncertainty presented by sediment redistribution and lack of submerged GPS stations. The majority of coastal regions including the Outer Banks and portions of southern Virginia show estimated subsidence on the order of 7–20 cm by 2100, which is consistent with both USGS and NOAA projections [7],[17].

Sea Level Rise Projections

As a result of a variety of greenhouse gas emissions scenarios, model uncertainty, and questions regarding the stability of the Antarctic and Greenland ice sheets, there remains a wide range in potential SLR realizations over the coming decades. Global mean sea levels are expected to increase on the order of 0.25 to 2 meters by the year 2100 [16],[17],[55],[56]. However, SLR is not regionally constant, with the Western Pacific and Western Atlantic experiencing more rapid increases [17],[57]. Along the Atlantic Coast, recent estimates extend from 0.3 m to >2.0 m in the event of high emissions and significant acceleration of glacial melt [15]-[17]. At sites specific to coastal North Carolina, NOAA projections display a similar range SLR scenarios (Table 1). Predictions from NOAA [17] account for land movement, thus considering relative SLR and tend to be slightly higher than those estimated by Hall et al. [16]. The high and low end of the presented ranges are unlikely, as one assumes no acceleration in the rate of SLR and others consider rapid glacial melt coupled with ice sheet collapse and increased thermal expansion. Projections in the middle to low end of this range thus provide reasonable estimates in line with anticipated increases in global mean sea levels and encompass the most likely scenarios. As such, three SLR approximations of 44, 55, and 74 cm were selected for use in ADCIRC simulations. Although the potential exists for true SLR above 0.44 - 0.74 m, these provide a realistic range of SLR increases captured within the scope of the most probable Representative Concentration Pathways (RCPs).

Table 1 – Sea level rise projections for 2100

Location	Projected Land Movement	Low	Intermediate	High	Source
Chesapeake Bay Bridge-Tunnel, VA	–	0.48 m	1.25 m	2.18 m	[16]
	0.16 – 0.20 m	0.44 m	1.18 m	2.59 m	[17]
Wilmington, NC	–	0.16 m	0.93 m	1.86 m	[16]
	0.03 – 0.07 m	0.32 m	1.02 m	2.46 m	[17]
Beaufort, NC	–	0.21 m	0.96 m	1.90 m	[16]
	0.07 – 0.12 m	0.36 m	1.09 m	2.54 m	[17]
Oregon Inlet Marina, NC	–	0.23 m	0.99 m	1.92 m	[16]
Southport, NC	–	0.17 m	0.93 m	1.86 m	[16]
Cape Hatteras, NC	0.11 – 0.17 m	0.40 m	1.13 m	2.36 m	[17]
Duck Pier, NC	0.13 – 0.18 m	0.41 m	1.16 m	2.59 m	[17]

Hurricane Simulations

Hurricane Irene made landfall in the Outer Banks near Cape Lookout, NC on August 27, 2011, bringing significant storm surge and wave action [28]. While Hurricane Matthew did not directly make landfall in the study region, it approached the coast before veering out to sea on October 10, 2016 (Fig. 3). Both events affected the region with hurricane force winds, with maximum sustained winds on the order of 130 – 140 km/h (approximately 84 mph). Fig. 3 details the storm path and extension of hurricane force and tropical storm force winds from the storm center. While both events crossed the study region with similar strengths, Irene proved to be a direct hit to much of the APES region. Counterclockwise wind circulation pushed sound side water inland and Atlantic waters towards the barrier islands before causing a seaward storm surge towards the sound-side Outer Banks as the system progressed in a northeasterly direction.

ADCIRC simulations are forced with ECMWF atmospheric pressure and wind fields. In a recent study by Garzon et al. [58], ECMWF was shown to most effectively model storm surges in the Chesapeake Bay in a comparison between six unique forcing data sets. In this study, ECMWF based forcing inputs remain unchanged across each set of simulations for both Irene and Matthew. Baseline simulations rely on up-to-date bathymetry and elevation models, land cover, and ECMWF meteorological parameters. Following baseline and validation runs, node elevations and water level datum are adjusted in the ADCIRC modeling framework to account for subsidence and SLR. Each storm was modeled with five unique simulations, including current day, subsidence only, and subsidence + SLR (of 44, 55, 74 cm) projections. The resulting node-specific maximum depths and hourly water level outputs were recorded over the duration of study periods for both Irene (August 26, 2011 – August 29, 2011) and Matthew (October 7, 2016 – October 10, 2016).

Results And Discussion

Model Validation for Irene and Matthew

Here, baseline simulations provide estimates of storm surge extent and water levels due to Hurricane Matthew and Irene as they made landfall. Using USGS gauge stations along the North Carolina Atlantic coast (Fig. 1), we validated water level observations against simulations to characterize model performance (Fig. 4). The resulting baseline simulations provide a reasonable origin point from which to compare future storm surge simulations to for the year 2100, as additional flooding due to land subsidence and rising seas can then be isolated.

Simulated water levels present strong agreement with observations with an RMSE ranging from 10 – 31 cm and an average correlation across all sites of greater than 0.8 (Fig. 4). Validation results also suggest acceptable performance in the modeling of storm surge temporal characteristics, as the timing of water level peaks and troughs are shown to be in good agreement both for tidal and storm surge dominant periods. The results suggest sufficient skill at modeling peak water levels for both events at the Duck and Beaufort observing sites, having errors within 5 cm for both storm events. However, significant underestimation in peak water levels was shown at both Hatteras and Oregon Inlet on the order of 0.3 - 0.5 meters. Both of these recording sites are situated on the sound side of the barrier islands, adjacent to more complex topographic features, highlighting the challenges of accurately modeling water levels in these areas compared to sites situated off the coast. Still, ADCIRC simulations model water levels with good accuracy, especially for Hurricane Irene, with RMSE's below 18 cm at all validation sites and very high correlations ($R^2 > 0.92$). Simulated water levels for Hurricane Matthew were not as accurate (RMSE 19 – 31 cm). Significant flooding due to rainfall also occurred during Hurricane Matthew which was not considered within the model framework. This may contribute to model underestimation of peak water levels, especially at Hatteras and Oregon Inlet gauges. Contributions from rainfall, riverine influences, errors in ECMWF wind forcing, and slight mismatches in initial node water depths (potentially due to dredging) all contribute to model uncertainty. Cassalho et al. [32] provide further model performance and validation statistics using both an assessment of high-water marks (USGS) and modeled wave heights. The study identifies model tendencies to underestimate high-water marks by around 0.5 meters which should be considered as a potential source of underestimation in surge projections.

Spatially (*see Supplementary information*), flood waters are simulated to inundate over 2,100 km^2 for Hurricane Irene and 1,400 km^2 for Matthew with much of this area being part of the P-AP. This is equivalent to an estimated 350 billion (Irene) and 140 billion gallons (Matthew) of water forced overland. For Hurricane Irene, severe flooding occurred in the southern APES with flood depths approaching and exceeding 1 meter in areas including Lowland, Stumpy Point, and over much of the central Outer Banks. In contrast, Hurricane Matthew produced more significant flooding towards the northern portion of the APES. This region is also characterized by an extensive area with elevations below 2 meters and gentle ground slopes which is shown to contribute to an increased duration of flood water retention following the initial storm surge. Overall, storm surge flooding due to Matthew was generally less severe than that of Irene. Still, both events placed substantial populations in the APES region within the maximum flood extent boundary including around 8,000 (Matthew) and 30,000 (Irene) individuals, based on data from the 2010 U.S. Census [18]. Estimates of flood extent are comparable to maximum inundation depths from hindcasts developed as part of the Coastal Emergency Risks Assessment (CERA) project (https://cera.coastalrisk.live, [59]) and NWS modeled flood extents [60]. Thus, model baseline simulations provide an adequate representation of storm impacts in regard to both flood extent and depth and provide a new perspective on the extent of at-risk populations living directly within the storm surge boundary.

The Relative Impacts of Subsidence and Sea Level Rise on Storm Surge

Hurricane Irene

Fig. 5 presents results in terms of spatial extent of maximum flood waters across the APES for Hurricane Irene. Where water levels at specified nodes (Bodie Island, Stumpy Point, Lowland) are presented to facilitate comparison. Subsidence alone is shown to increase the extent of flooded area by 27% relative to present day conditions. This increase exposes an additional estimated 5,000 individuals [18] to flooding for an event similar to Hurricane Irene. While notable differences are observed considering only land movement, with the addition of SLR, potential impacts become especially destructive. Even considering a low SLR scenario (+44 cm), by 2100 the flood extent of a storm similar to Irene is expected to nearly double (increase by 87%) placing upwards of 100,000 people at risk in the APES region alone. In the highest modeled scenario (+74 cm) the areal extent of flooding nears 5,000 km^2, an increase of 127% compared to baseline simulations. Worsening surges are shown to be focused over the P-AP, which is especially at risk of regular inundation due to its low elevation profile.

Results suggest that approximately half of the P-AP can expect inundation by a storm event equivalent to Hurricane Irene. In comparing the rate of growth in the flooded area, the no-SLR to +44 cm scenario produces an increase in flood extent by 60% (1,309 km^2), while the additional flood extent in comparing +44 cm to +74 cm of SLR increases by only 40% (878 km^2). Proving the susceptibility of this region to even modest SLR, while suggesting the extent of flooding may increase non-linearly. Predicted increases in inundation are also prevalent over the southern half of the Outer Banks. Remarkably, at and around Bodie Island, an increase in both the duration and expanse of inundation is anticipated, though modeled overland depths are shown to decrease relative to both subsidence only and baseline simulations. This result is counterintuitive, as SLR and land movement are shown to result in reduced overland flood depths at many locations. We hypothesize this is due to a more expansive inundation area, as water spreads out over the coastal plain reducing the mean storm surge depths. This redistribution of flood waters is shown at both Bodie Island and Lowland nodes. However, locally high land elevations in close proximity to Stumpy Point Bay result in increased storm surge depths as local topography results in increased surge backups in this area.

SLR also contributes to a significant shift in storm surge temporal characteristics not seen in subsidence only simulations (Fig. 5). Specifically, SLR simulations predict delayed peak flood timings and increasing flood durations. These results illustrate the complex dynamics between the land surface and storm surge, as increases in maximum flood depths assume a non-linear relationship with SLR. Additionally, many locations are predicted to become part of the tidal basin even in normal conditions (e.g., Lowland and Stumpy Point), which exposes a considerable area to regular tidal flooding. This will have serious implications to property damage as well as coastal erosion. Overall, while subsidence will contribute to a rise in coastal flooding, SLR is the driving force in worsening hurricane events across coastal North Carolina.

Hurricane Matthew

In Fig. 6 we compare the expected contributions of land subsidence and SLR to increases in flood extent using Hurricane Matthew as the underlying meteorologic forcing. Increases in sea level and decreases in land surface elevations result in flooded areas similar to Irene, but with even more striking increases compared to the baseline simulation. Due to settlement alone, we estimate a more than 40% (+607 km^2) increase in flood extent relative to the baseline (Table 2). Still, SLR is shown to be the primary driver of increases in the regional extent of storm surge. Fig. 6 illustrates an increased area exposed to storm surge flooding on the order of 3x the baseline extent in the most severe scenario simulations (+74 cm SLR), expanding by upwards of 240% from 1,431 km^2 to 4,939 km^2. In this scenario, the areal extent of inundation is almost identical to that of Hurricane Irene considering +74 cm SLR (4,982 km^2). Highlighting the susceptibility of these areas to storm surge with the expectation of more frequent flooding even considering a variety of storm characteristics (i.e., varied wind fields, approach angles). Here results show substantial increases in flood risk in the Outer Banks as well, directly contributing to the considerable rise in affected populations. SLR drives the transition from affecting only sparsely populated areas (~8,000 residents) to more than 115,000 within APES region alone.

Future simulations also resulted in similar peak water level timing at the Hobucken and Hatteras nodes compared to baseline simulations, with a general delay in maximum flood depth timing on the order of 2 hours. In contrast, at Gum Neck which is located at low elevations on the P-AP, we see a considerable delay in peak surge timing. Flood waters are simulated to rise steadily and drain slowly over this area, largely due to topography, as much of the additional simulated flood area is situated below 0.5 m (Fig. 1). Still, the increases in flood depths are not anticipated to be as extreme in the region surrounding the Alligator River such as other non-protected areas (e.g., Hobucken and Hatteras). In Gum Neck, surge depths are shown to remain within 25 cm of baseline projected maximum depths, even when considering SLR considerably exceeding this amount (>44 cm). This is relative to more exposed locations, where additional wind water interaction and more severe surges are expected. Inundation at Hatteras is shown to increase substantially with the max flood depths rising by nearly 1 m when considering +74 cm of SLR compared to the baseline. Over both Hatteras and Hobucken nodes, flood duration as a result of Matthew is shown to increase substantially. Our results indicate that much of the low-lying portions of the P-AP and those south of the Pamlico River will be reclaimed by the sound in coming decades due to SLR, becoming uninhabitable as they transition into part of the tidal basin.

Discussion, Significance, and Study Limitations

SLR is revealed to provide the dominant contribution to increased storm surge flood extents, with increases on the order of 90% to 250% compared to around 30% to 40% in subsidence only simulations (Table 2). This indicates that while land movement is expected to result in significant increases in coastal areas at risk of flooding, SLR is anticipated to be the primary driver of the burgeoning storm surge flood risk across the APES. Still, outcomes from this study suggest that both land movement and SLR should be considered when estimating implications of future coastal storm events. Furthermore, as a direct result of these factors, a similar increase in the size of populations exposed to storm surges in many coastal communities is anticipated. In the more severe projections, which consider 74 cm of SLR coupled with land subsidence, over 100,000 additional individuals are likely to be impacted in the region. In the case of Hurricane Matthew, an increase of over 1,400%.

Table 2 – ADCIRC simulation summary statistics for shown APES region. Areal overland extent determined as areas with positive water depths over the land surface as defined by the present-day DEM. Vulnerable population statistics derived from CIESIN 2017 datasets (2010 U.S. Census) [18]

-	Simulation	Flood Depth (m)			Flooded Area			Vulnerable Population
		Mean	Median	Standard Deviation	Areal Extent	Additional Impacted	Flood Extent Increase (%)	
Irene	Baseline - 2011	0.63	0.55	0.37	2196 km^2	–	–	28,513
	Sub. Only – 2100	0.66	0.58	0.37	2795 km^2	599 km^2	27%	33,713
	Sub. + SLR (44 cm) - 2100	0.56	0.46	0.42	4104 km^2	1908 km^2	87%	102,523
	Sub. + SLR (55 cm) - 2100	0.63	0.54	0.44	4454 km^2	2258 km^2	103%	111,370
	Sub. + SLR (74 cm) - 2100	0.74	0.67	0.47	4982 km^2	2787 km^2	127%	133,568
Matthew	*Baseline - 2016*	0.39	0.34	0.21	1431 km^2	–	–	8,214
	Sub. Only – 2100	0.44	0.41	0.21	2038 km^2	607 km^2	42%	13,278
	Sub. + SLR (44 cm) - 2100	0.49	0.45	0.30	4052 km^2	2621 km^2	183%	79,428
	Sub. + SLR (55 cm) - 2100	0.56	0.53	0.33	4395 km^2	2964 km^2	207%	93,575
	Sub. + SLR (74 cm) - 2100	0.68	0.67	0.37	4939 km^2	3508 km^2	245%	115,328

Previous efforts to understand the regional susceptibility to climate change and potential impacts have been made, with comparable findings to that of this work. Over the P-AP prior investigations have suggested that 1 m of SLR could inundate over 40% of the region, having disproportionate impacts on poor communities [22]. Even further, a global analysis of populations at risk to 0.9 m SLR in 2016 identified over 90,000 residents expected to be at risk in coastal NC by 2100 considering current populations and 165,000 considering population growth rates [25]. These efforts present a range comparable to projections of at-risk populations considering SLR and storm surges here, of approximately 80,000 to 130,000 residents. These estimates are based on current populations and would increase if considering expected population growth.

The North Carolina Climate Science Report [61] identifies increases in heavy precipitation (very likely), significant SLR (virtually certain), increased hurricane intensity (medium confidence), and required changes in associated engineering design standards (very likely) as ongoing or probable effects of climate change. To quantify expected impacts of SLR, Kopp et al. [15] estimated significant increases in the frequency of severe coastal flooding to occur between 2050 and 2100, depending on RCPs. As a result, an estimated >$4 and $17 billion of additional coastal properties will experience regular flooding by 2050 and 2100, respectively [62]. Combining our efforts with findings from such studies suggests that at a decadal timescale, large portions of the region will become unlivable due to more severe and frequent flooding. The results also suggest that even events that provide a glancing blow to the region (Matthew) could have impacts similar to that of a direct hit (Irene) in the future. This is most notable in comparing maximum flood extents in +74 cm SLR simulations in which the extent of inundated areas converged towards 5,000 km^2. This suggests topographic characteristics in the region that may slow the growth of at-risk areas in the event of additional SLR. Subsequently, storm surge flooding will take a pronounced toll on agriculture and ecosystems in the APES, especially within the P-AP. The region may no longer be able to support soybean, corn, and logging industries due to the combined effects of subsidence and SLR. The effects of these factors, accelerated by coastal storm events, will reshape the APES along with the communities and ecosystems within it. Likely implications identified here reiterate those identified by Poultera et al. [63], with additional ecological impacts due to saltwater intrusion, wetland accretion, barrier island section collapse, and loss of waterfront property. Many of these changes may come more rapidly than most are aware. Risk reduction policies including investment in engineered protections, relocation programs, and flood insurance should be employed.

Multiple considerations and limitations are important to consider. First, there remains uncertainty regarding the maximum water level projections due to known model underestimation of high-water marks. Hydrologic inputs from riverine models and contributions due to rainfall are also largely ignored here, which can be expected to contribute to increased flooding across the APES. The lack of available information on the true areal extent of flooding from both Hurricane Irene and Matthew also limits validation of baseline surge estimates. FEMA estimates suggest damages due to Hurricane Matthew were more costly to North Carolina with nearly $400 million in federal assistance allocated [64] compared to Irene in which approximately $140 million was allocated [65]. Hurricane Matthew damaged or destroyed over 98,000 homes, 19,000 businesses, and a considerable amount of infrastructure (e.g., roads, dams) suggesting underestimation of affected populations by this study [66]. This may be due in part to the use of outdated population statistics (2010), however, request for federal aid also incorporate damages due to high winds and riverine flooding statewide. The proportion of damages contributed by storm surge are nearly impossible to determine, complicating model validation. More severe surges were observed during Irene compared to Hurricane Matthew, even as total damages remained significantly lower. This suggests that the relative contribution of storm surge to total event damages was considerably larger in the case of Irene. Finally, SLR projections are in line with the lower end of guidance and contain a considerable amount of uncertainty. The range used here (44 cm - 74 cm) encompasses a few possible scenarios, however different carbon emissions pathways and stability of the Antarctic and Greenland ice sheets will largely determine the rate at which SLR is realized. Other notable projections [67] paint a dire picture of global SLR by 2100 increasing globally up to 1.4 m relative to 1990. Rahmstorf [67] also asserts that long term records indicate that in order to achieve global equilibrium, total SLR may be closer to 10 meters per 1 °C of warming. With global mean temperatures having already warmed by 1 °C since 1880, this would engulf much of the APES coastline and Outer Banks when considering a timescale of thousands of years. For these reasons, SLR scenarios as part of this study can be considered to be conservative, suggesting that the true effects of future hurricane events may be even more devastating to the region.

Conclusions

Numerical modeling presents an effective method for estimating and projecting storm surges and their impacts into the future. In this paper, we utilize the ADCIRC modeling framework to quantify additional storm surge related effects of two recent hurricane events (Irene and Matthew) considering both land subsidence and sea level rise (SLR) across the Albemarle-Pamlico Estuary System. Using estimates for year 2100, we examine the areal extent, at-risk populations, as well as flood timing and depth changes associated with subsidence and SLR. The results show that while land movement contributes to a significant increase in the areal extent exposed to storm surge flooding (+ 27% and + 40%), SLR is expected to remain the primary driver of worsening storm surge impacts for coastal North Carolina. For Irene, the combination of land settlement and 74 cm of SLR resulted in an increase in the storm surge-prone area from around 2,196 km^2 to nearly 5,000 km^2 (+ 127%). In the case of Matthew, simulations showed an even more devastating increase in flooded areas, with a nearly 250% increase in flood extent (1,431 km^2 to 4,939 km^2). As a result, large increases in affected populations are predicted with over 100,000 additional residents being exposed to flooding when comparing 2100 scenarios to baseline storm simulations in coastal North Carolina alone. With the duration of storm surge inundation also shown to increase, additional erosion and property damage will be increasingly likely. Interestingly, the results also suggest that while flood depths are anticipated to increase, this does not occur equivalent to the amount of

SLR. As model results show much of the additional water is expected to spread out over a considerably larger area resulting in a relationship between increasing storm surge depths and SLR that is non-linear and location dependent. This is in contrast to the projected increase in surge depth due to land subsidence alone which displays a more predictable linear rate of increase. Most importantly, our results illustrate that by 2100 markedly more severe storm surges can be expected from hurricanes of equivalent intensity today, even considering relatively conservative estimates of SLR and low-end hurricane events. As a result, we expect worsening flood impacts in terms of more frequent and damaging outcomes to populations, coastal ecosystems, and infrastructure. In response, efforts should be employed such as engineered flood protections, relocation, and land use planning to limit losses in the coming decades.

Declarations

Acknowledgements

The authors want to thank the Texas Advanced Computing Center (TACC) of The University of Texas at Austin for providing the High-Performance Computing resources necessary. In this work, we utilized the Extreme Science and Engineering Discovery Environment (XSEDE) STAMPEDE2 resources through allocation id TG-BCS130009, which is supported by National Science Foundation [grant number ACI-1548562].

Author Contributions

All authors contributed to the study conception and design. Computational simulations were performed by Felicio Cassalho and Jeremy Johnston. Material preparation, data collection and analysis were performed by Jeremy Johnston, Felicio Cassalho, and Tyler Miesse. Manuscript drafts were written by Jeremy Johnston and all authors made editorial contributions on each draft. All authors read and approved the final manuscript.

Additional Information

Competing interests statement: The authors declare no competing interests as defined by Nature Research, or other interests that might be perceived to influence the results and/or discussion reported in this paper.

Availability of data and material: Derived subsidence maps and maximum flood extent raster files from each of the simulations as GeoTIFFs. Raw simulation outputs as netCDF (.nc) files are available upon request from fcassalh@gmu.edu. ECMWF ERA5 forcing inputs are available via Copernicus at https://cds.climate.copernicus.eu/cdsapp#!/dataset/reanalysis-era5-single-levels?tab=form.

References

1. Peltier, W. R. Global glacial isostasy and the surface of the Ice-age Earth: The ICE-5G (VM2) Model and GRACE. Annual Review of Earth and Planetary Sciences 32, 111–149 (2004).
2. Karegar, M. A., Dixon, T. H. & Engelhart, S. E. Subsidence along the Atlantic Coast of North America: Insights from GPS and late Holocene relative sea level data. Geophysical Research Letters 43, 3126–3133 (2016).
3. Sun, H., Grandstaff, D. & Shagam, R. Land subsidence due to groundwater withdrawal: potential damage of subsidence and sea level rise in southern New Jersey, USA. Environmental Geology 37, 290–296 (1999).
4. Galloway, D., Jones, D. R. & Ingebritsen, S. Land Subsidence in the United States. U.S. Geological Survey Circular USGS Circ. 1182, (1999).
5. Zervas, C. Sea level variations of the United States, 1854–2006. https://repository.library.noaa.gov/view/noaa/2565 (2009).

6. Ezer, T. & Atkinson, L. P. Accelerated flooding along the U.S. East Coast: On the impact of sea-level rise, tides, storms, the Gulf Stream, and the North Atlantic Oscillations. Earth's Future 2, 362–382 (2014).
7. Eggleston, J. & Pope, J. Land subsidence and relative sea-level rise in the southern Chesapeake Bay region: U.S. Geological Survey Circular 1392. 30 (2013).
8. Loftis, J. D. et al. Communities and Areas at Intensive Risk in the Mid-Atlantic Region: A Reanalysis of 2011 Hurricane Irene with Future Sea Level Rise and Land Subsidence. in OCEANS 2018 MTS/IEEE Charleston 1–7 (2018). doi:10.1109/OCEANS.2018.8604864.
9. Miller, M. M. & Shirzaei, M. Land subsidence in Houston correlated with flooding from Hurricane Harvey. Remote Sensing of Environment 225, 368–378 (2019).
10. Phien-wej, N., Giao, P. H. & Nutalaya, P. Land subsidence in Bangkok, Thailand. Engineering Geology 82, 187–201 (2006).
11. Rodolfo, K. S. & Siringan, F. P. Global sea-level rise is recognised, but flooding from anthropogenic land subsidence is ignored around northern Manila Bay, Philippines. Disasters 30, 118–139 (2006).
12. Abidin, H. Z., Andreas, H., Gumilar, I. & Wibowo, I. R. R. On correlation between urban development, land subsidence and flooding phenomena in Jakarta. in Proceedings of the International Association of Hydrological Sciences vol. 370 15–20 (Copernicus GmbH, 2015).
13. Kulp, S. A. & Strauss, B. H. New elevation data triple estimates of global vulnerability to sea-level rise and coastal flooding. Nature Communications 10, 4844 (2019).
14. Kirezci, E. et al. Projections of global-scale extreme sea levels and resulting episodic coastal flooding over the 21st Century. Scientific Reports 10, 11629 (2020).
15. Kopp, R. E., Horton, B. P., Kemp, A. C. & Tebaldi, C. Past and future sea-level rise along the coast of North Carolina, USA. Climatic Change 132, 693–707 (2015).
16. Hall, J.A. et al. Regional Sea Level Scenarios for Coastal Risk Management: Managing the Uncertainty of Future Sea Level Change and Extreme Water Levels for Department of Defense Coastal Sites Worldwide. U.S. Department of Defense, Strategic Environmental Research and Development Program. 224. (2016).
17. Sweet, W.V. et al. Global and Regional Sea Level Rise Scenarios for the United States (No. NOS CO-OPS 083), NOAA Technical Report. National Oceanic and Atmospheric Administration. (2017). https://tidesandcurrents.noaa.gov/publications/techrpt83_Global_and_Regional_SLR_Scenarios_for_the_US_final.pdf
18. Center for International Earth Science Information Network (CIESIN), Columbia University. U.S. Census Grids (Summary File 1), 2010. Palisades, NY: NASA Socioeconomic Data and Applications Center (SEDAC). (2017). doi: 10.7927/H40Z716C
19. FitzGerald, D. M., Fenster, M. S., Argow, B. A. & Buynevich, I. V. Coastal Impacts Due to Sea-Level Rise. Annual Review of Earth and Planetary Sciences 36, 601–647 (2008).
20. Titus, J. G. et al. State and local governments plan for development of most land vulnerable to rising sea level along the US Atlantic coast. Environ. Res. Lett. 4, 044008 (2009).
21. Michael, H. A., Post, V. E. A., Wilson, A. M. & Werner, A. D. Science, society, and the coastal groundwater squeeze. Water Resources Research 53, 2610–2617 (2017).
22. Bhattachan, A. et al. Sea level rise impacts on rural coastal social-ecological systems and the implications for decision making. Environmental Science & Policy 90, 122–134 (2018).
23. Tully, K. et al. The Invisible Flood: The Chemistry, Ecology, and Social Implications of Coastal Saltwater Intrusion. BioScience 69, 368–378 (2019).
24. Neumann, B., Vafeidis, A. T., Zimmermann, J. & Nicholls, R. J. Future Coastal Population Growth and Exposure to Sea-Level Rise and Coastal Flooding - A Global Assessment. PLOS ONE 10, e0118571 (2015).

25. Hauer, M. E., Evans, J. M. & Mishra, D. R. Millions projected to be at risk from sea-level rise in the continental United States. Nature Climate Change 6, 691–695 (2016).
26. Mudd, L., Wang, Y., Letchford, C. & Rosowsky, D. Assessing Climate Change Impact on the U.S. East Coast Hurricane Hazard: Temperature, Frequency, and Track. Natural Hazards Review 15, 04014001 (2014).
27. Vidon, P. et al. In the path of the Hurricane: impact of Hurricane Irene and Tropical Storm Lee on watershed hydrology and biogeochemistry from North Carolina to Maine, USA. Biogeochemistry 141, 351–364 (2018).
28. Avila, L. & Cangialosi, J. Hurricane Irene Tropical Cyclone Report (No. AL092011). NOAA. (2011). https://www.nhc.noaa.gov/data/tcr/AL092011_Irene.pdf
29. Stewart, S. Hurricane Matthew Tropical Cyclone Report (No. AL142016). NOAA. (2017). https://www.nhc.noaa.gov/data/tcr/AL142016_Matthew.pdf
30. Wang, J., Gao, W., Xu, S. & Yu, L. Evaluation of the combined risk of sea level rise, land subsidence, and storm surges on the coastal areas of Shanghai, China. Climatic Change 115, 537–558 (2012).
31. Sebastian, A. et al. Characterizing hurricane storm surge behavior in Galveston Bay using the SWAN + ADCIRC model. Coastal Engineering 88, 171–181 (2014).
32. Cassalho, F. et al. Coastal Wetlands Exposure to Storm Surge and Waves in the Albemarle-Pamlico Estuarine System during Extreme Events. Wetlands 41, 49 (2021).
33. Peng, M., Xie, L. & Pietrafesa, L. J. A numerical study of storm surge and inundation in the Croatan–Albemarle–Pamlico Estuary System. Estuarine, Coastal and Shelf Science 59, 121–137 (2004).
34. Xia, M., Xie, L., Pietrafesa, L. J. & Peng, M. A Numerical Study of Storm Surge in the Cape Fear River Estuary and Adjacent Coast. coas 24, 159–167 (2008).
35. Rueda, A. et al. A global classification of coastal flood hazard climates associated with large-scale oceanographic forcing. Sci Rep 7, 5038 (2017).
36. Cyriac, R. et al. Variability in Coastal Flooding predictions due to forecast errors during Hurricane Arthur. Coastal Engineering 137, 59–78 (2018).
37. N.C. Division of Marine Fisheries. NCDEQ - NCDMF Harvest Statistics. http://portal.ncdenr.org/web/mf/marine-fisheries-catch-statistics
38. Copeland, B. J. & Gray, J. Status and Trends of the Albemarle-Pamlico Estuaries, Albemarle-Pamlico Estuarine Study Report 90 – 01 (Dept. of Environment, Health & Natural Resources, Raleigh, NC, 1991)
39. Paerl, H. W. et al. Ecosystem impacts of three sequential hurricanes (Dennis, Floyd, and Irene) on the United States' largest lagoonal estuary, Pamlico Sound, NC. PNAS 98, 5655–5660 (2001).
40. Lagomasino, D., Corbett, D. R. & Walsh, J. P. Influence of Wind-Driven Inundation and Coastal Geomorphology on Sedimentation in Two Microtidal Marshes, Pamlico River Estuary, NC. Estuaries and Coasts 36, 1165–1180 (2013).
41. Clunies, G. J., Mulligan, R. P., Mallinson, D. J. & Walsh, J. P. Modeling hydrodynamics of large lagoons: Insights from the Albemarle-Pamlico Estuarine System. Estuarine Coastal and Shelf Science 189, 90–103 (2017).
42. Paerl, H. W. et al. Ecological response to hurricane events in the Pamlico Sound system, North Carolina, and implications for assessment and management in a regime of increased frequency. Estuaries and Coasts: J ERF 29, 1033–1045 (2006).
43. Luettich, R. A., Carr, S. D., Reynolds-Fleming, J. V., Fulcher, C. W. & McNinch, J. E. Semi-diurnal seiching in a shallow, micro-tidal lagoonal estuary. Continental Shelf Research 22, 1669–1681 (2002).
44. Mulligan, R. P., Walsh, J. P. & Wadman, H. M. Storm Surge and Surface Waves in a Shallow Lagoonal Estuary during the Crossing of a Hurricane. Journal of Waterway, Port, Coastal, and Ocean Engineering 141, A5014001 (2015).
45. Luettich, R. A., Westerink, J. J. & Scheffner, N. W. ADCIRC: An Advanced Three-Dimensional Circulation Model for Shelves, Coasts, and Estuaries. Report 1. Theory and Methodology of ADCIRC-2DDI and ADCIRC-3DL. US Army Corps

of Engineers (USACE) 143 (1992).

46. Booij, N., Ris, R. C. & Holthuijsen, L. H. A third-generation wave model for coastal regions: 1. Model description and validation. Journal of Geophysical Research: Oceans 104, 7649–7666 (1999).
47. Xie, D., Zou, Q. & Cannon, J. W. Application of SWAN + ADCIRC to tide-surge and wave simulation in Gulf of Maine during Patriot's Day storm. Water Science and Engineering 9, 33–41 (2016).
48. Blanton, B. et al. Urgent Computing of Storm Surge for North Carolina's Coast. Procedia Computer Science 9, 1677–1686 (2012).
49. National Geophysical Data Center. U.S. Coastal Relief Model - Southeast Atlantic. National Geophysical Data Center, NOAA. (1999). doi:10.7289/V53R0QR5.
50. Cooperative Institute for Research in Environmental Sciences (CIRES) at the University of Colorado, Boulder. Continuously Updated Digital Elevation Model (CUDEM) – 1/9 Arc-Second Resolution Bathymetric-Topographic Tiles. NOAA National Centers for Environmental Information. (2014). doi: 10.25921/ds9v-ky35.
51. GEBCO Bathymetric Compilation Group. The GEBCO_2020 Grid - a continuous terrain model of the global oceans and land. British Oceanographic Data Centre, National Oceanography Centre, NERC, UK. doi:10/dtg3. (2020).
52. Jin, S. et al. Overall Methodology Design for the United States National Land Cover Database 2016 Products. Remote Sensing 11, 2971 (2019).
53. Liu, H., Zhang, K., Li, Y. & Xie, L. Numerical study of the sensitivity of mangroves in reducing storm surge and flooding to hurricane characteristics in southern Florida. Continental Shelf Research 64, 51–65 (2013).
54. Hersbach, H. et al. The ERA5 global reanalysis. Quarterly Journal of the Royal Meteorological Society 146, 1999–2049 (2020).
55. Rahmstorf, S. A new view on sea level rise. Nature Climate Change 1, 44–45 (2010).
56. Oppenheimer, M. et al. Sea Level Rise and Implications for Low-Lying Islands, Coasts and Communities. in IPCC Special Report on the Ocean and Cryosphere in a Changing Climate. In press. (2019).
57. Rietbroek, R., Brunnabend, S.-E., Kusche, J., Schröter, J. & Dahle, C. Revisiting the contemporary sea-level budget on global and regional scales. PNAS 113, 1504–1509 (2016).
58. Garzon, J. L., Ferreira, C. M. & Padilla-Hernandez, R. Evaluation of weather forecast systems for storm surge modeling in the Chesapeake Bay. Ocean Dynamics 68, 91–107 (2018).
59. Fleming, J. G. et al. A Real Time Storm Surge Forecasting System Using ADCIRC. 893–912. (2012). doi:10.1061/40990(324)48.
60. Bandy, R., Newport, W. & City, M. Communicating with Maps and Graphics – NWS Products and Services (PowerPoint Slides). *National Weather Service*. 49. (2012)
61. Kunkel, K.E. et al. North Carolina Climate Science Report. North Carolina Institute for Climate Studies, 233. https://ncics.org/nccsr (2020).
62. Houser. 4. U.S. CLIMATE PROJECTIONS. Economic Risks of Climate Change 23–38 (Columbia University Press, 2015).
63. Poultera, B. et al. Sea-level rise research and dialogue in North Carolina: Creating windows for policy change. Ocean & Coastal Management 52, 147–153 (2009).
64. FEMA. North Carolina Hurricane Matthew (DR-4285-NC) | FEMA.gov. https://www.fema.gov/disaster/4285 (2016).
65. FEMA. North Carolina Hurricane Irene (DR-4019-NC) | FEMA.gov. https://www.fema.gov/disaster/4019 (2011).
66. Cooper, R. State of North Carolina Supplemental Request for Assistance: Hurricane Matthew Recovery. 9 (2017).
67. Rahmstorf, S. A Semi-Empirical Approach to Projecting Future Sea-Level Rise. Science 315, 368–370 (2007).

Figures

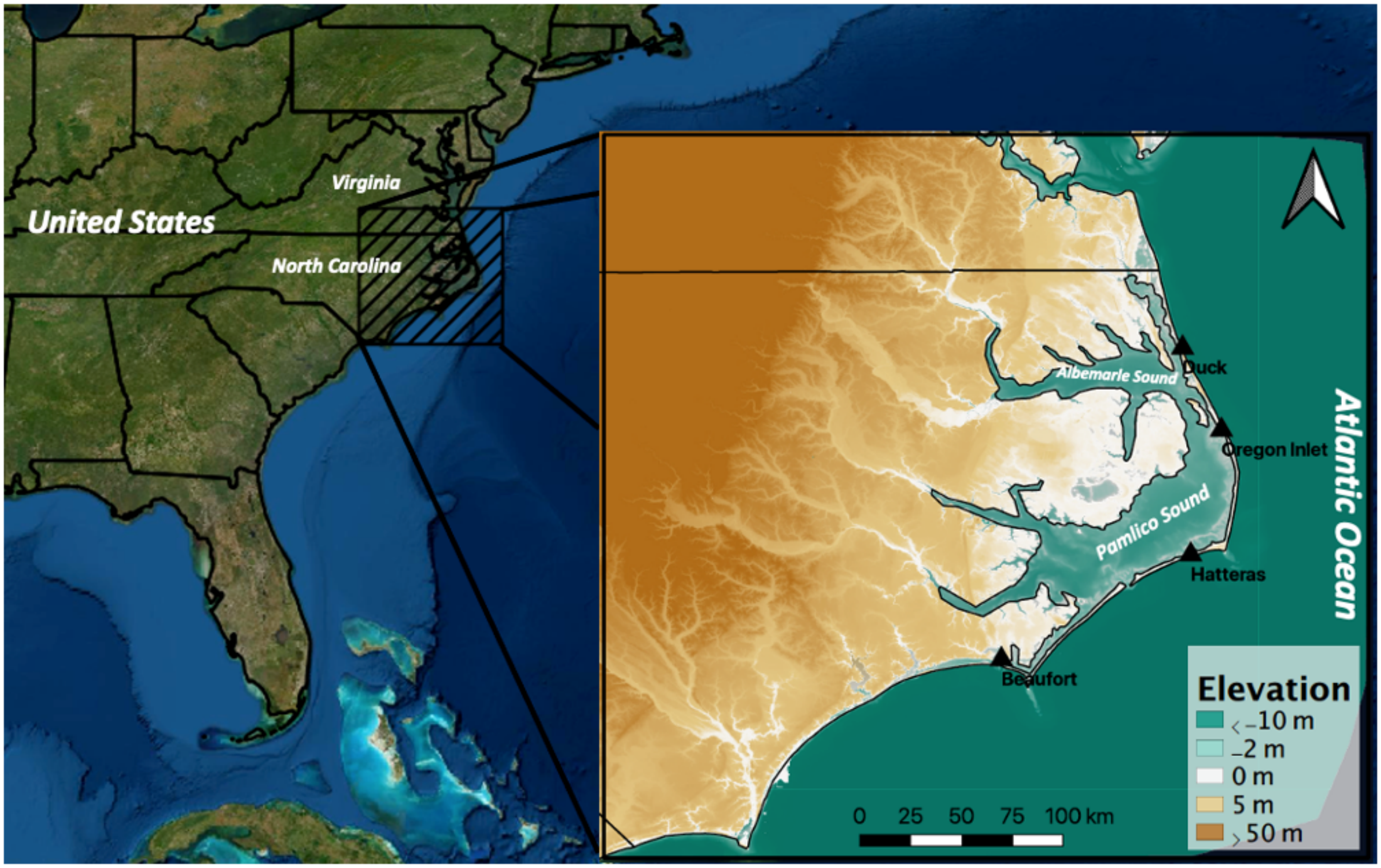

Figure 1

Study region with elevation and bathymetry (CUDEM, Coastal Relief Model, GEBCO, USGS). Water level recording stations indicated. Note: The designations employed and the presentation of the material on this map do not imply the expression of any opinion whatsoever on the part of Research Square concerning the legal status of any country, territory, city or area or of its authorities, or concerning the delimitation of its frontiers or boundaries. This map has been provided by the authors.

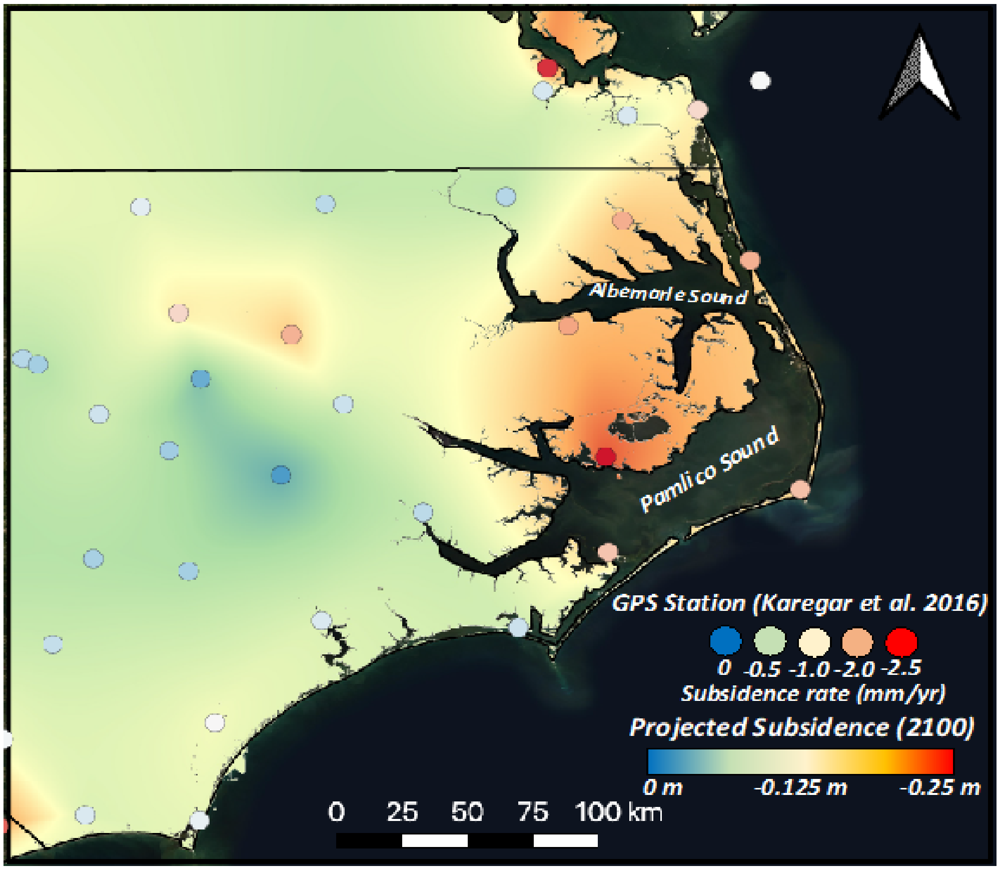

Figure 2

Annual subsidence rates and GPS recording stations (from [2]) and projections of total land surface elevation changes by 2100. Note: The designations employed and the presentation of the material on this map do not imply the expression of any opinion whatsoever on the part of Research Square concerning the legal status of any country, territory, city or area or of its authorities, or concerning the delimitation of its frontiers or boundaries. This map has been provided by the authors.

Storm	Intensity	Max Wind Speed (km/h)	Minimum Pressure (mb)
Irene (2011)	Category 1	139	952
Matthew (2016)	Category 1	130	983

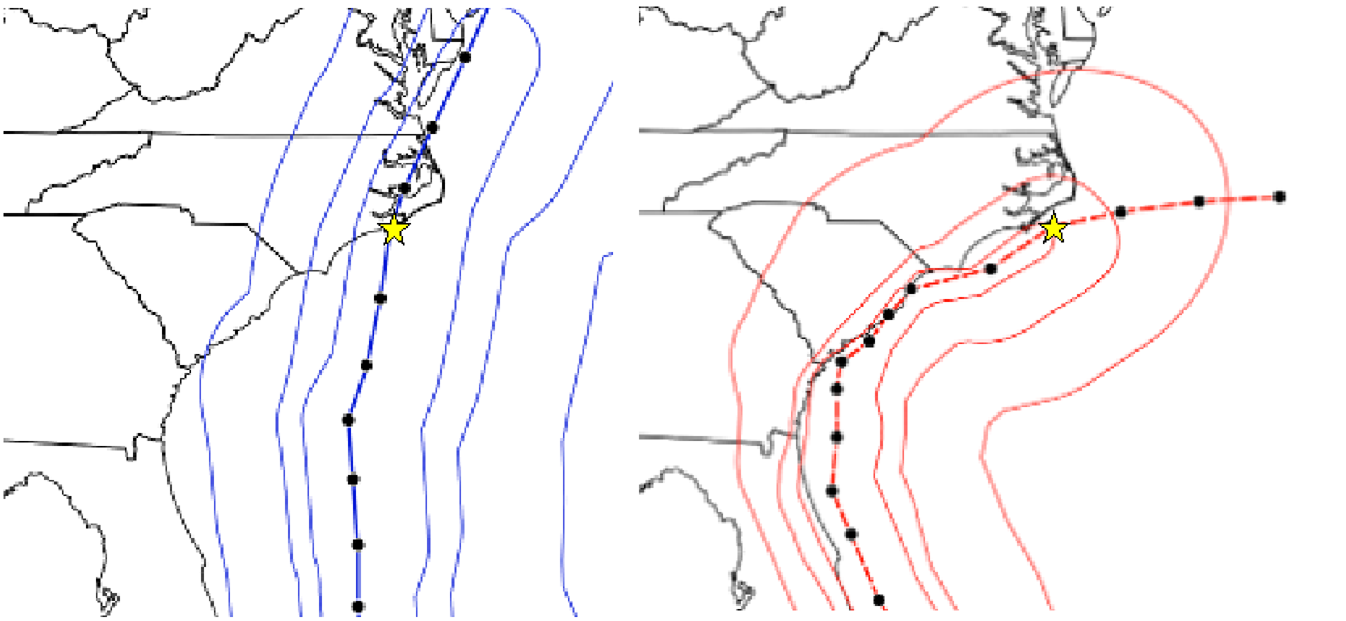

Irene (8/26/2011 - 8/28/2011) Matthew (10/7/2016 - 10/10/2016)

Figure 3

Best track and wind field indicated for hurricanes Irene and Matthew. Wind speed and pressure characteristics recorded for position nearest landfall in North Carolina (indicated by star). Best track information available via the National Hurricane Center, https://www.nhc.noaa.gov/gis/. Note: The designations employed and the presentation of the material on this map do not imply the expression of any opinion whatsoever on the part of Research Square concerning the legal status of any country, territory, city or area or of its authorities, or concerning the delimitation of its frontiers or boundaries. This map has been provided by the authors.

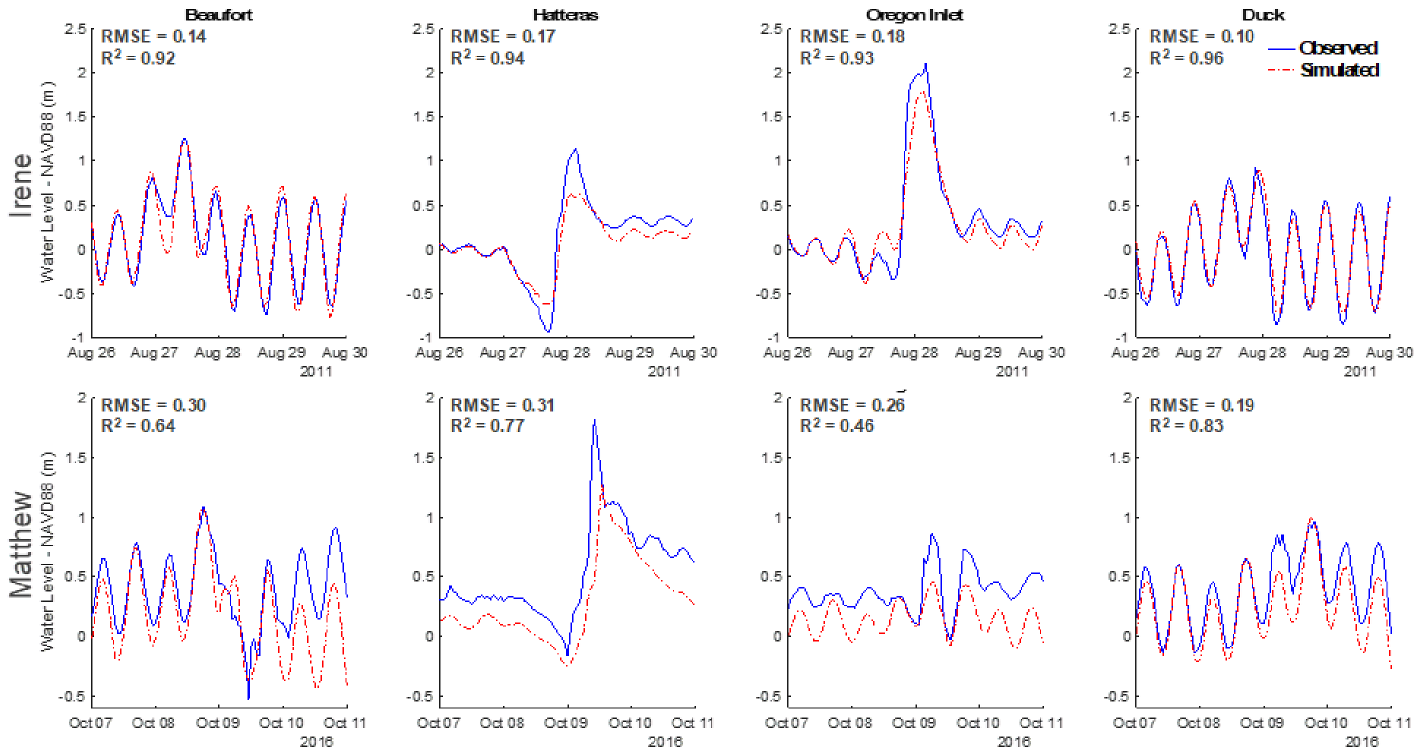

Figure 4

Model validation against NOAA water level gages. RMSE and correlations computed across near storm periods, Irene (August 26 0Z – August 30 0Z) and Matthew (October 7 0Z – October 11 0Z)

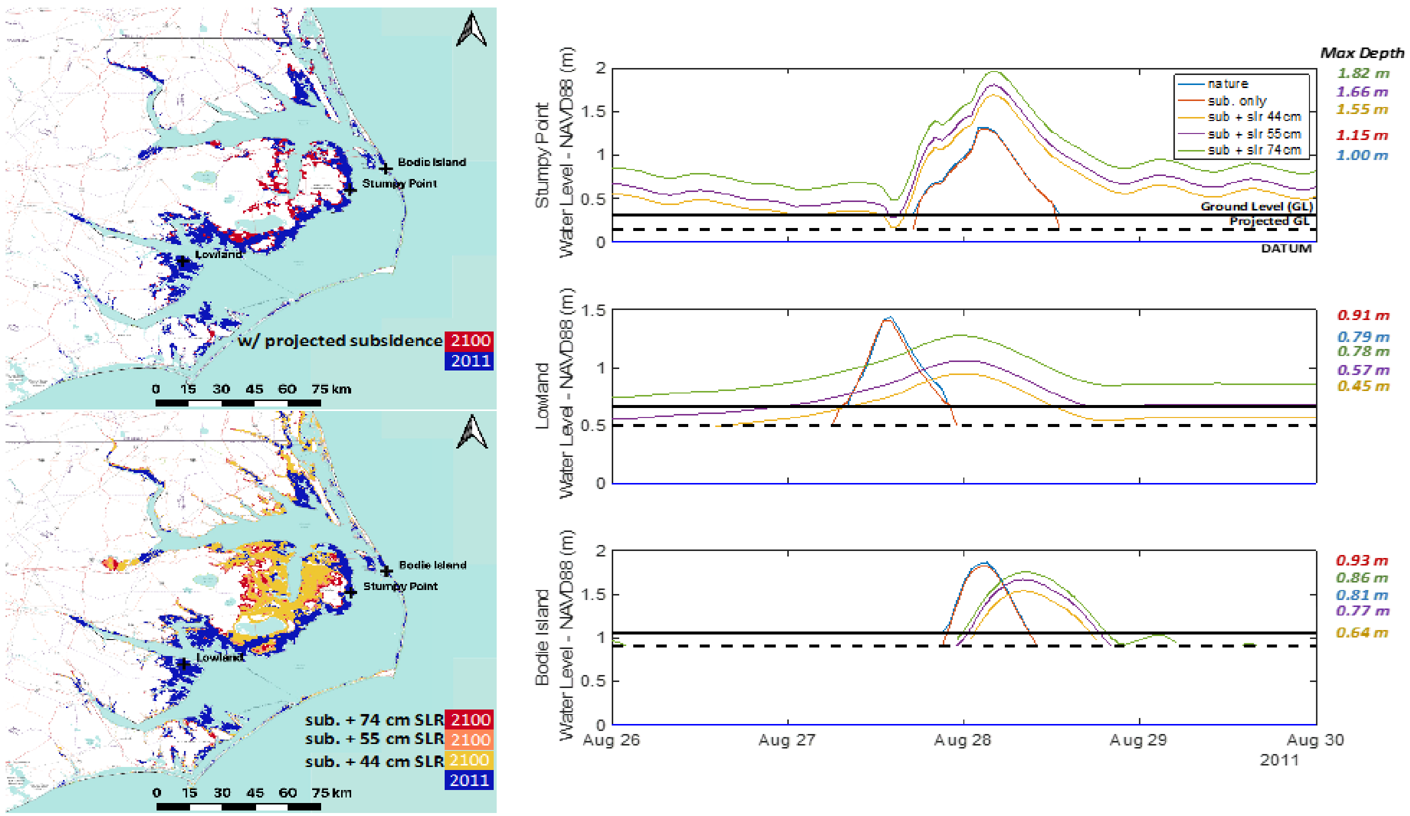

Figure 5

Hurricane Irene flood extent and water level timeseries at indicated focus node locations including Bodie Island, Stumpy Point, and Lowland, NC. Results summarized in Table 2. Note: The designations employed and the presentation of the material on this map do not imply the expression of any opinion whatsoever on the part of Research Square concerning the legal status of any country, territory, city or area or of its authorities, or concerning the delimitation of its frontiers or boundaries. This map has been provided by the authors.

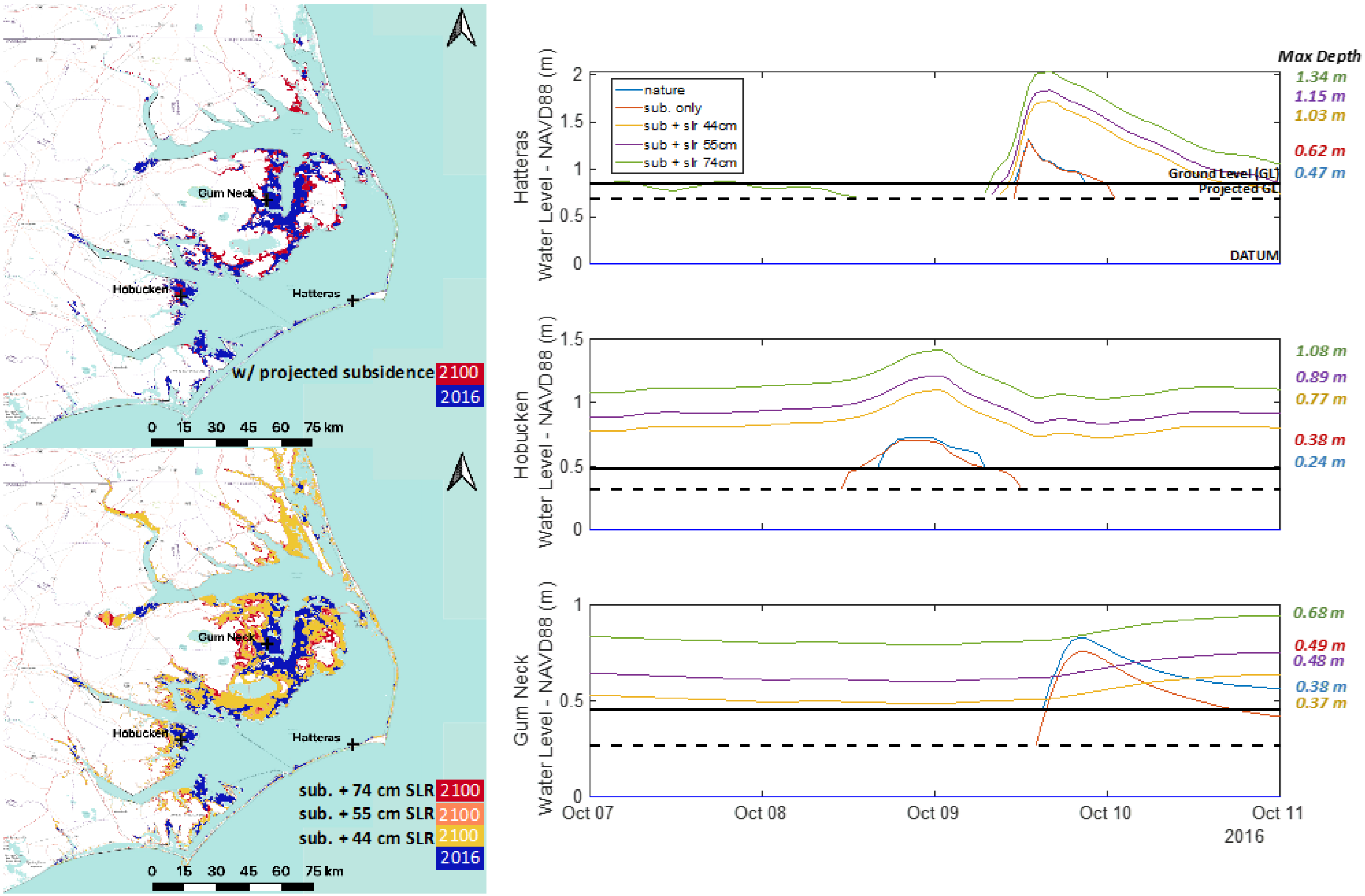

Figure 6

Hurricane Matthew flood extent and water level timeseries at indicated focus node locations including Gum Neck, Hobucken, and Hatteras, NC. Results summarized in Table 2. Note: The designations employed and the presentation of the material on this map do not imply the expression of any opinion whatsoever on the part of Research Square concerning the legal status of any country, territory, city or area or of its authorities, or concerning the delimitation of its frontiers or boundaries. This map has been provided by the authors.

Supplementary Files

This is a list of supplementary files associated with this preprint. Click to download.

- BaselineSimulationsInundationMap.tiff
- SupplementaryInfoSubsidenceProject.docx